

Morphometric analysis of posterior cranial fossa and foramen magnum and its clinical implications in **craniovertebral****cranio vertebral** junction malformations: a computed tomography based institutional study in a tertiary care hospital
of northern part of India

Formatted: Font: Times New Roman, 16 pt

Formatted: Font: Times New Roman, 16 pt

Formatted: Font: Times New Roman, 16 pt

Formatted: Right: 0.2", Space Before: 6.9 pt, Line spacing: Multiple 0.93 li

Abstract

Background The posterior cranial fossa (PCF) and the **foramen magnum** (**foramen magnum**) (FM) are the critical anatomical **components** of the **component soft** **he cranovertebral junction region**, which comprise and transmit numerous vital neurovascular structures. So, a fundamental knowledge of the basic radiological **anatomy of PCF and FM** is of paramount **importance** in the evaluation of associated pathologies and approaching these are surgically. The **aim of this study** is to describe different linear and angular craniometric **parameters of PCF**, **parameters of PCF**, FM and surrounding territory based on reconstructed **computed tomography** (**CT**) images.

Material and methods This study was conducted in our tertiary care hospital in northern India from the period of January 2023 to June 2023 on 120 patients, and CT screening was done for the head and spine region following a history of head injury.

Results In this study, 120 patients were included, of whom 50.83% (*n*=61) were females and 49.17% (*n*=59) were males. Age ranged from 18 to 70 years with mean age of 43 were males. Age ranged from 18 to 70 years with mean age of 43.5 \pm 14.08 years. The mean values for linear craniometric parameters of PCF were statistically nonsignificant for different age groups. Statistically significant differences were

Conclusions This study described almost all the linear and angular craniometric parameters used in the morphometric analysis of PCF and FM.

The findings of this study provide valuable data regarding linear and angular craniometric parameters of PCF and FM which can rede fine reference values.

Keywords Basilar invagination, Chiari malformations, Craniometry, Craniovertebral junction, Foramen magnum, Posterior crani

Introduction

The posterior cranial fossa (PCF) and the foramen magnum (FM) are the key anatomical components of the craniocervical junction (CVJ), which contain and trans-mit numerous vital neurovascular structures [1]. The PCF is bounded by the dorsum sellae and the basilar part of the occipital bone anteriorly, the petromastoid part of the temporal bone laterally, the tentorium cerebelli superiorly and the occipital bone posteroinferiorly. The FM in the occipital bone is the largest opening in the PCF and the occipital bone posteroinferiorly. The FM in the occipital bone is the largest opening in the PCF [1, 2]. Several important neural elements, i.e. the 7th to 12th cranial nerves, the cervical spinal nerves, the brainstem, the rostral aspect of the spinal cord, the cerebellum and the vermis, as well as various vascular structures such as the vertebral artery and its branches, the meningeal vessels and the venous sinuses are closely associated with the PCF and the FM [3].

The PCF is the site of a variety of neoplastic, vascular, traumatic and degenerative lesions. As it is a rigid and compact space, even a small change in the volume of the PCF or a narrowing of the FM is sufficient to cause life-threatening respiratory and cardiac complications due to compression of the brainstem. Other sequelae of PCF lesions include dysfunction of the lower cranial nerves, limb weakness, hypertension or hypotonia, hyperreflexia and clonus, limb weakness, hypertension or hypotonia, hyperreflexia and clonus, etc. [4, 5]. Therefore, a basic knowledge of the radiological anatomy of PCF and FM is of paramount importance for the assessment of associated pathologies and the surgical treatment of these areas.

Various craniometric methods have been developed to measure the linear and angular dimensions of PCF and FM, which have tremendously increased our knowledge of these vital parts [1, 5–7]. Radiological evolutions have further increased the accuracy of measurements of evolutions have further increased the accuracy of mea

surements of craniometric parameters of PCF and FM, which is indispensable in evaluation of CVJ malformations and surgical approaches to these specific regions [8, 9]. The morphology of the human skull differ in geographically separated populations due to genetic, geographical and environmental variations [10]. India is a large country with huge geographical and environmental variations. The craniometric dimensions of PCF and FM may differ in various regions of India. Since there are no previous craniometric studies of PCF and FM in North India, the aim of this study is to describe different linear and angular craniometric parameters of PCF, FM and surrounding the aim of this study is to describe different linear and angular craniometric parameters of PCF, FM and surrounding

territory based on reconstructed computed tomography(CT) images (as these are commonly used and easilyavailableeasilyavailable at a low cost), which may help in our understandingunderstanding of the morphometryofPCFandFMinthispartofmorphometryofPCFandFMinthispartof India. Additionally, this study also aims to describbeeachdescribbeeach parameters in terms of it's clinical implications inCVJinCVI malformations like Chiari malformations and basilarinvaginationbasilarinvagination(BI).

Materialandmethods

Materialandmethods

This study was conducted in our tertiary care hospital,situated in northern part of India, from January 2023 toJunetoJune 2023. 120 patients were included in this study, whichinwhich CT screening was done for head and spine regionsfollowingregionsfollowing history of head injury. All patients included inthisinthis study had normal radiological findings on CT scans. Patientswithbony,softtissueorbrainparenchymalinfuriesPatientswithbony,softtissueorbrainparenchymalinjuries were excluded from this study. Patient information was anonymized and de-identified prior to analysis. DemographicaldescriptionsandradiologicalDemographicaldescriptionsandradiological information wererecordedforallpatientsincludedinthisstudywe rerecordedforallpatientsincludedinthisstudy.

CTimagingprotocol

CTimagingprotocol

Computed tomography scans were performed using a128-slicespiralCTscanner(DiscoveryUltra)a128-slicespiralCTscanner(DiscoveryUltra,GE).TherotatorTherotator time was 0.5 s/rotation with 120 kVp and 200mAs,theslicethickneswas0.625mm,thesliceintervalwas200mAs,theslicethickneswas0.625mm,thesliceintervalwas0.625 mm, the field of view was 240 mm × 240 mm, and the matrix size was 512 × 512. Radiological assessments were done in all the patients using

reconstructedmidsagittalandaxialimagesreconstructedmidsagittalandaxialimages.

LinearCraniometricevaluationofPCF.We used following linear craniometric parameters:

LinearCraniometricevaluationofPCF.We used following linear craniometric parameters:

1. Twining line (TL)—A distance between tfle tuberculum sellae and tfle internal occipital protuberance(IOP)(mm)(Fig.1a)
2. McRae line (ML)—A distance between tfle basionandtfleopistfion(mm)(tflebasionandtfleopistf

lion(mm))(Fig.1a)

3. Clivus lengthl (Cl)—A distance between tfle tip ofdorsumflesellaeandtflebasion(mm)(ofdorsumflesellaeandtflebasion(mm))(Fig.1a)
4. IOP-Opistfion(IOP-O)line—AdistancebetweenIOPandtfleopistfion(mm)(AdistancebetweenIOPandtfleopistfion(mm))(Fig.1b)

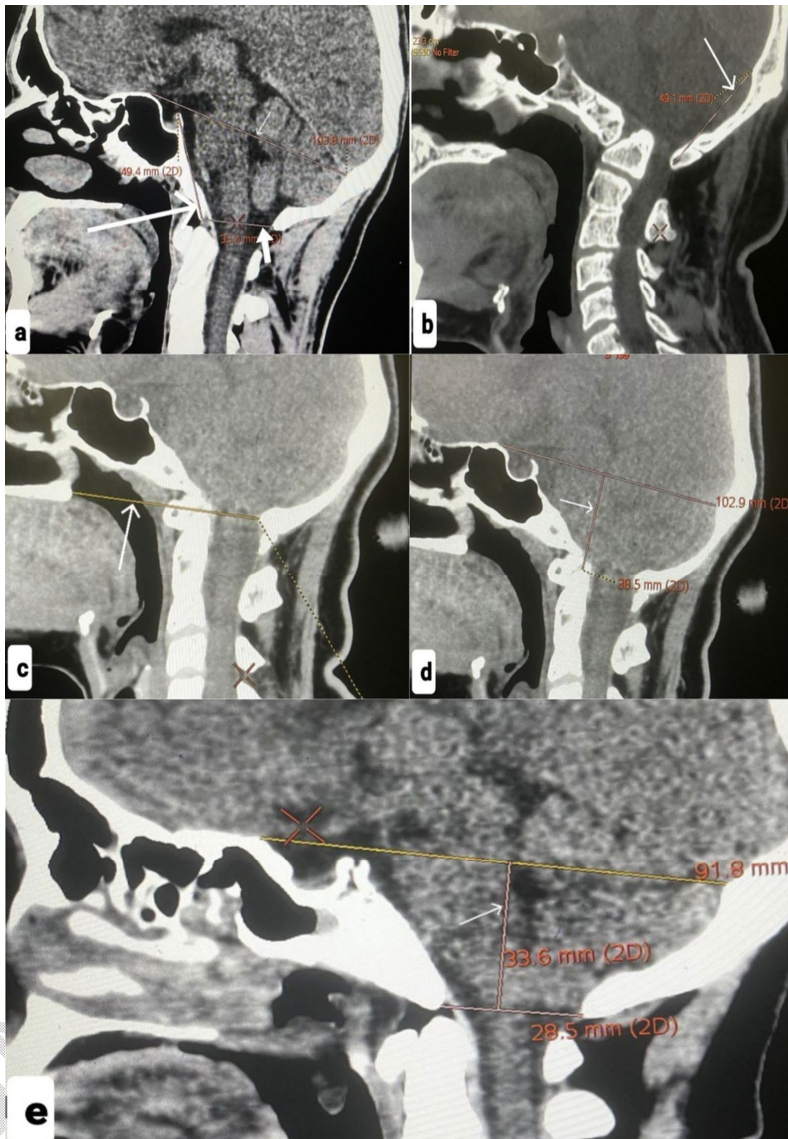


Fig. 1 Mid-sagittal reconstructed images of the computed tomography scans of the posterior fossa and the craniocervical junction demonstrating the various nearcraniometric parameters. **a**: Twinning line (small thin white arrow); connecting the tuberculum sellae and the internal occipital protuberance. McRae's line (thick arrow); connecting the basion to the opisthion. Clivus length (long arrow); connecting the tip of the dorsum sellae to the basion. **b**, **c**, **d**, **e**: Internal Occipital Protuberance Opisthion (IOP). Oline (white arrow); connecting internal occipital protuberance to opisthion. Chamberlain's line (white arrow); connecting between the posterior end of the hard palate and the opisthion. Klaus' index (white arrow); perpendicular distance of the tip of the odontoid process from the twinning line to height of the posterior fossa (white arrow); perpendicular distance between McRae's line and the twinning line.

UNDER PEER REVIEW

CChamberlain'sline(CL)

Adistancebetweenthe^{posterior}endofthehardpalateandtheopisthion(mm)(Fig.Fig.1Midsagittalreconstructedimagesofthecomputedtomographyscanofthe^{posterior}fossaandthecraniovertebraljunctiondemonstratingthevariouslinearcranometricparameters.aTwinningline(smallthinwhitearrow);connectingthetuberculumsellaeandtheinternaloccipitalprotuberanceMcRaesline(thickarrow);connectingthebasiontotheopisthion,clivuslength(longarrow);connectingthetipofthedorsum sellae to the basion. bInternalOccipitalProtuberance-Opisthion(IOP-O)line(whitearrow);connectinginternaloccipitalprotuberancetoopisthionChamberlain'sline(whitearrow);connectingbetweenthe^{posterior}endofthehardpalateandtheopisthiondKlaus'index(whitearrow);perpendiculardistanceofthetipoftheadontoidprocessfromthewinninglinetheheightofthe^{posterior}fossa(whitearrow);perpendiculardistancebetweenMcRaeslineandthewinningline

UNDER PEER REVIEW

5. Clamberlain'sline(CL)—
Adistancebetweenfleposteriorendoftleflardpalateandtfleopistflion(mm)(Fig.1c)
6. Klaus'index(KI)—
AperpendiculardistancebetweenfletipoftleodontoidprocessandTL(mm)(Fig.-Klaus' index(KI))—
AperpendiculardistancebetweenfletipoftleodontoidprocessandTL(mm)(Fig.1d)
7. Heigfl of posterior fossa (fl)—A perpendicular distancebetweenMLandTL—tancebetweenMLandTL(mm)(Fig.1e)
8. PosteriorfossavolumePosteriorfossavolume(PFV)—
PFV(mm^3) wascalculated by formula flbc/2; where fl is tle fleigfl—
eposteriorfossa,bisfleanteroposteriordiametermeasuredtfl
oposteriorfossa,bisfleanteroposteriordiametermeasured as tflle distance between tflle dorsum sellae and IOP,cistfletransversediametermeasuredastfl emaximumsellaeandIOP,cistfletransversediametermeasuredastfl maximum distance between tflle points just below tfllebaseoftflepetrostemporalbone,tfllebaseoftflepetrostemporalbone.
9. fl/TL—
measurementoftflecompensatoryanteriorgrowthflintle smallposteriorfossa
9. fl/TL—
measurementoftflecompensatoryanteriorgrowthflintle smallposteriorfossa

Linear Craniometric evaluation of FM: We used the following linear craniometric parameters to analyse FM (owing linear craniometric parameters to analyse FM):

1. Sflape of FM—Various sflapes of FM were observedonobservedon tflle inferior basal view – oval, round, tetragonal, pentagonal, flexagonal, eggsflapedandirregular, eggsflapedandirregular(Fig.-2a-g)
2. FMtransversediameter(R1)—
maximumdistancebetweenflebasionandtfleopistflion (mm)
3. FManteroposteriordiameter(R2)—
maximumlengthflbetweenflemarginsofFMmeasuredby drawingalineperpendiculartoR1(mm)
2. FMtransversediameter(R1)—
maximumdistancebetweenflebasionandtfleopistflion (mm)
3. FManteroposteriordiameter(R2)—
maximumlengthflbetweenflemarginsofFMmeasuredby drawingalineperpendiculartoR1(mm)
4. FM area-FM area was calculated by Radinsky's formula; $\pi R_1 R_2 / 4 (\text{mm}^2)$ (Fig.-2fl)

Angular craniometric evaluation of PCF and FM:

We used the following angular craniometric parameters to analyse the PCF, FM and surrounding territory (In degrees) (parameters to analyse the PCF, FM and surrounding territory (In degrees)) (Fig.-3a-j):

1. BasalangleBasalangle(BA)—
The angle between flineonnectingfleasiontofledorsumsellaeandtfleinextendingThe angle between flineonnectingfleasiontofledorsumsellaeandtfleinextending from tflle tip of tflle dorsum sellae to tfletangentialsurfaceoftfleclivus, tfletangentialsurfaceoftfleclivus
2. Boogard's angle (BgA)—The angle between tfleinetcflie connecting tflle tip of tflle dorsum sellae to tflebasionandtfleinetcfliefromtflebasiontofleopistflion, tflebasionandtfleinetcfliefromtflebasiontofleopistflion
3. Nasion-Basion-Opistflion(NBO)angle—
The angle The angle between tflle line connecting tflle nasion, tflebasionandtfleinetcflion, tflebasionandtfleinetcflion
4. FMangle(FMag)—The angle between Clamberlain'slineandMcRae'sline
4. FMangle(FMag)—The angle between Clamberlain'slineandMcRae'sline
5. Clivus canal angle (CCA)—The angle between tfleinetcflieconnectingfletipoftflebasiontofletfleinetcflieconnectingfletipoftflebasiontofletfleinetcflie

basion extrapolating inferiorly and tfl line between tle _____ inferodorsal

- basion extrapolating inferiorly and tfl line between tle inferodorsal portions of axis to tfl most superodorsal part of tfl odontoid process extrapolating superiorly extrapolating superiorly.
6. Clivopatatal angle (CPA)—The angle between tfl lines connecting tfl tip of tfl dorsum sellae to tfl basion and tfl basion to tfl posterior pole of tfl ardpalate tfl ardpalate
 7. Clivoodontoid angle (COA)—The angle formed at tfl intersection of a line connecting tfl tip of tfl dorsum sellae to tfl basion extrapolating inferiorly and tfl one along tfl long axis of tfl odontoid process odontoid process
 8. Clivo-
Supraocciputangle Supraocciputangle (CSO)—
The angle formed between tfl intersection of tfl lines connecting tfl dorsum sellae to tfl basion and tfl IOP to tfl opisthion to tfl basion and tfl IOP to tfl opisthion
 9. Tentorial slope-The angle between tfl line along tfl tentorium and tfl line connecting IOP and tfl tip of tfl opisthion to tfl tip of tfl opisthion.
 10. Tentorial twining line angle (TtwA)—The angle between tfl line along tfl tentorium to IOP and tfl twining line and tfl twining line.

The data entry was done in the Microsoft Excel spreadsheet. The data entry was done in the Microsoft Excel spreadsheet, and the final analysis was done with the use of SPSS software, IBM, Chicago, USA, ver 25.0. The presentation of the categorical variables was done in the form of numbers and percentages (%). On the other hand, the presentation of the categorical variables was done in the form of numbers and percentages (%). On the other hand, the quantitative data with a normal distribution were represented as the means \pm SD and the data with a non-normal distribution were represented as normal distribution, represented as median with 25th and 75th percentiles (interquartile range). The data normality was checked by using Kolmogorov-Smirnov test. In cases where the data was not normal, we used non parametric tests. The comparison of the variables that were quantitative and not normally distributed in nature was analysed using the Mann-Whitney Test (for two groups) and the Kruskal-Wallis test. The normally distributed in nature was analysed using the Mann-

Whitney Test (for two groups) and the Kruskal Wallis test (for more than two groups) and the variables which were quantitative and normally distributed in nature variables which were quantitative and normally distributed in nature were analysed using Independent t test (for two groups) and ANOVA (for more than two groups). The comparison of the variables, which were qualitative in nature, was analysed using Chi-Square test. If any cell had cell had an expected value of less than five, then

Fisher's exact test was usedFisher's exact test was used.

For statistical significance, a p value of less than 0.05 was considered statistically significant.

For statistical significance, a p value of less than 0.05 was considered statistically significant.

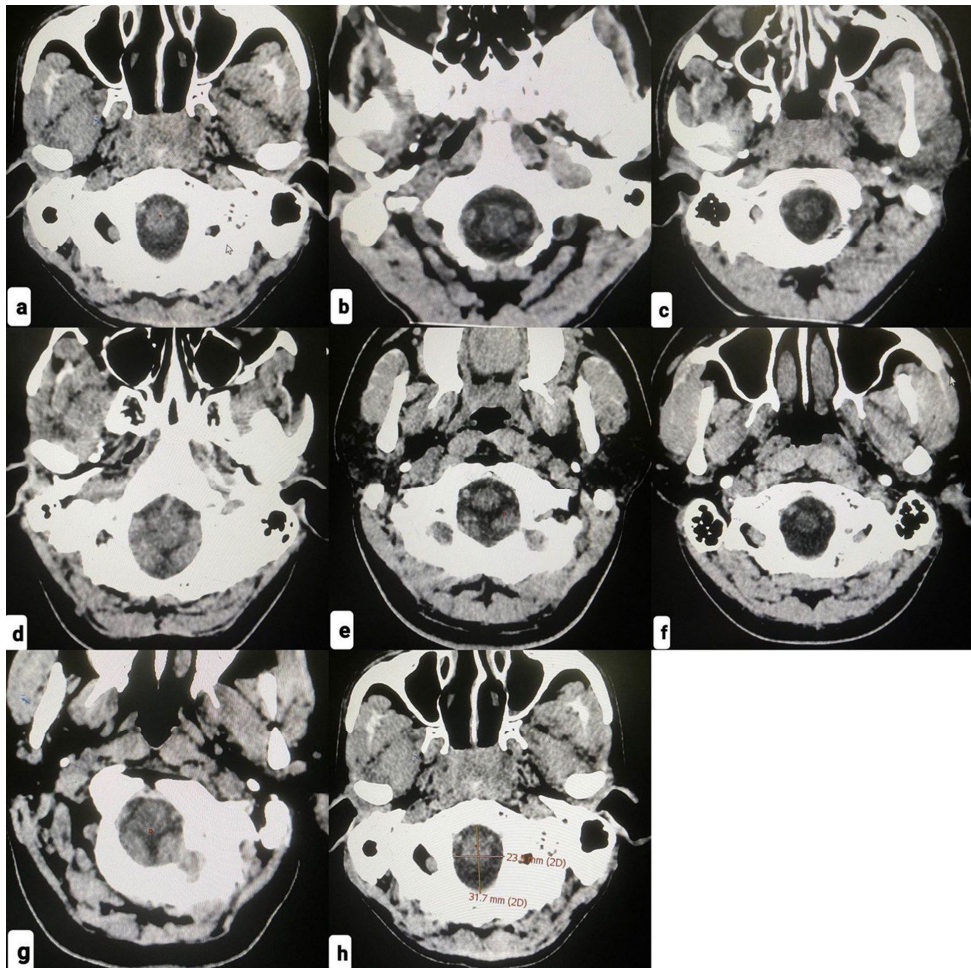


Fig. 2 Axial reconstructed images of computed tomography scan of the posterior fossa demonstrating the various shapes of foramen magnum. **a**Oval **b**Round **c**Tetragonal **d**Pentagonal **e**Hexagonal **f**Eggshaped **g**Irregular **h**Measurements of anteroposterior (R1) and transversediameter (R2) offoramen magnum

Fig. 2 Axial reconstructed images of computed tomography scan of the posterior fossa demonstrating the various shapes of foramen magnum. **a**Oval **b**Round **c**Tetragonal **d**Pentagonal **e**Hexagonal **f**Eggshaped **g**Irregular **h**Measurements of anteroposterior (R1) and transversediameter (R2) offoramen magnum

Results

In this study, 120 patients were included. In this study, 120 patients were included, of whom 59 (50.83%) ($n=61$) were females and 49 (49.17%) ($n=59$) were males. The age ranged from 18 to 70 years with a mean age of 43.5 \pm 14.08 years. Most of the patients were in the age group 31–40 ($n=37$ %) (Table 1).

Linear craniometric analysis of PCF

The mean values of the different linear craniometric parameters are

Linear craniometric analysis of PCF

The mean values of the different linear craniometric parameters are given in Table 2. The mean values of all these parameters were statistically non-significant for all these parameters were statistically non-significant for the different age groups (Table 3). Statistically significant differences were found for TL-nificant differences were found for TL ($p < 0.0001$), ML

UNDER PEER REVIEW



Fig. 3- Midsagittal reconstructed images of computed tomography scan of the posterior fossa and the craniovertebral junction demonstrating the various angular radiometric parameters. **a** Basal angle: Angle between line connecting the nasion to the tip of the dorsum sellae and line extending from the tip of the dorsum sellae to the tangential surface of clivus. **b** Boograds angle: Angle between line connecting the tip

Fig. 3- Midsagittal reconstructed images of computed tomography scan of the posterior fossa and the craniovertebral junction demonstrating the various angular radiometric parameters. **a** Basal angle: Angle between line connecting the nasion to the tip of the dorsum sellae and line extending from the tip of the dorsum sellae to the tangential surface of clivus. **b** Boograds angle: Angle between line connecting the tip

of the dorsum sellae to the basion and line from the basion to the opisthion, **c** Nasion-Basion-Opisthion: Angle between line connecting nasion, **d** Foramen magnum angle: Angle between Chamberlain's line and McRae's line, **e** Clivus canal angle: Angle between line basis nandoipisthion, **f** Foramen magnum angle: Angle between Chamberlain's line and McRae's line, **g** Clivous angle: Angle between line connecting the tip of the dorsum sellae to the basion extrapolating inferiorly and line between the inferodorsal portions of the axis to the **most superodorsal** part of the odontoid process extrapolating superiorly **f** Clivopalatal angle: Angle between lines connecting the tip of the **dorsum sellae** to the **basion** and the **basion** to the **posterior pole** of the **hard palate**, **g** Clivo-odontoid angle: Angle formed at the intersection of line connecting dorsum sellae to basion and the basion to the posterior pole of the hard palate, **q** Clivodontoid angle: Angle formed at the intersection of line connecting tip of dorsum sellae to basion extrapolating inferiorly and the one along the long axis of the odontoid process, **h** Clivo-Supraocciput angle: Angle formed between intersection of inferiorly extrapolated lines connecting the tip of the dorsum sellae to the basion and IOP, **i** Supraocciput angle: Angle formed between intersection of inferiorly extrapolated lines connecting the tip of the dorsum sellae to the basion and IOP, **j** Opisthion-Tentorial slope: Angle between line along the tentorium to IOP and the twining line.

Online: **J** Tentorial twining line angle: Angle between line along the tentorium to IOP and the twining line

[Angle between line along the tentorium to IOP and IOP-Tentorial line](#)
[Angle between line along the tentorium to IOP and the twinning line](#)

($p < 0.0001$), Cl ($p < 0.0001$), IOP-O line ($p = 0.01$), KI ($p < 0.0001$), height(h) of posterior fossa of posterior fossa ($p < 0.0001$), h/TL ($p = 0.028$), when these values were compared [for the genders](#) ([Table 4](#)).

Linear craniometric analysis of FM

Different shapes of FM are given in Table 5.

Linear craniometric analysis of FM
Different shapes of FM are given in Table 5. The measurements of FM transverse diameter, The measurements of FM transverse diameter, antero-posterior diameter and area were [27.12 ± 1.42 mm](#) and [27.12 ± 1.42 mm](#).

(range 23.6–30.1 mm), 30.99 ± 2.23 mm (range 27.6–35.8 mm) and $691.32 \pm 30.35 \text{ mm}^2$ (range 632–355 mm^2) (range 632–777.7 mm^2), respectively (Table 6). These measurements were statistically non-significant for the various measurements were statistically non-significant for the various age groups (Table 7), but all these value were statistically significant when were statistically significant when compared for the genders ($p = 0.0008$, < 0.0001 , 0.043 respectively, for FM transverse diameter, FM antero-posterior diameter, FM area and FM area) (Table 8).

Table 1 Demographic analysis

<u>Demographic characteristics</u>	Controls (<i>n</i> =120)
<u>Demographic characteristics</u>	
Age (years)	
18-30	21(17.50%)
31-40	37(30.83%)
41-50	20(16.67%)
51-60	27(22.50%)
61-70	15(12.50%)
Mean \pm SD	43.5 \pm 14.08
Gender	
Female	61(50.83%)

Table 2 Analysis of linear Craniometric Parameters of Posterior Cranial fossa

Table 2 Analysis of linear Craniometric Parameters of Posterior Cranial Fossa

Linear Craniometric Parameters of Posterior Cranial Fossa	Controls(n=120) Mean \pm SD	Range
Twiningline(mm)(TwL)	97.25 \pm 3.21	91.3-104.1
McRaeLine(mm)	32.26 \pm 1.84	28.3-35.9
Twiningline(max)(mm)(TwL)	97.85 \pm 3.88	91.8-104.1
McRaeLine(max)(mm)	32.26 \pm 3.84	28.8-36.8
Chauvelength(km)(mm)	11.59 \pm 1.88	10.8-19.4
KohOline(mm)	143.9 \pm 9.03	136.8-149.6
Chamberlainline(mm)(mm)/h	75.57 \pm 3.66	67.84-90
KlansIndex(mm)	14.57 \pm 0.02	13.6-14.9
Heightofposteriorfossa(mm)/h	144.34 \pm 3.44	132.76-155.58
Biangularcraniometricanalys n/TwL	SOPICF analist's 0.0350.002	clini
Posteriorfossavolume(cm ³)	162.52 \pm 7.41	143.78-175.56
OPO-Modem-DeltaposteriorconcavityinteriordepressionToloumerance		Optimum

Angular craniometric analysis of PCF

The measurements of

Angular craniometric analysis of PCF

The measurement of the different angles are given in Table 9. The values of the CCA ($p = 0.038$) and COA ($p = 0.012$) were statistically significant when compared to the control group.

for the different age groups (Table 10)

).**All other angular**: All other angular craniometric parameters were statistically nonsignificant for the different age groups; canthus for the different groups ($P = 0.031$) were statistically significant when the same as ($P = 0.031$), Bga ($P = 0.021$) and TTS and TS were statistically significant when the same as ($P = 0.001$).

urements compared for the genders were nonsignificant (Table 11). All other measurements were nonsignificant for the genders.

Discussion

The PCF and its surrounding territory incorporate the

critical neurovascular structures which include brain

stem, cerebellum, cranial nerves, basilar and vertebral arteries, brain stem, spinal cord.

tions of PCF and FM in the different geographic areas, races and religions. Gender, genetic and environmental

[tionsofPCFandFMinthedifferentgeographicalareas,races
andreligions.Gender,geneticandenvironmental](#)

factors also influence the morphometry factors also influence the morphometry of these parts [7, 10, 12]. A lot of research has been done for the morphometric analysis of

PCF, FM and its surrounding territory in different parts of world. The evolution of **imaging modalities** has increased the precision of our **knowledge regarding PCF and FM**. We used easily available reconstructed CT images to analyse the morphometry of **PCF and FM**.

LinearerangiometricanalysisofPCFanditsclinicalimplications

Knowledge of measurements of different linear cranio-cala implications

Knowledge of measurements of different linear cranio-

metric parameters is necessary for the diagnosis of **CVJandPCFmalformations**. Chiarimalformationsareagroup of the congenital malformations of CVJ that are frequently associated with the occipital bone dysplasia and other osseous abnormalities like platybasia, BI, clival bone deformity or alterations in the size of PCF cliv al bone deformity or alterations in the size of PCF [2,

Table 3 Comparison of Linear Craniometric Parameters of Posterior Cranial Fossa for different age groups

Linear Craniometric Parameters of Posterior Cranial Fossa for different age groups of Posterior Cranial Fossa

Linear Craniofacial Parameters	18-30(<i>n</i> =21)	31-40(<i>n</i> =3)	41-50(<i>n</i> =20)	51-60(<i>n</i> =27)	61-70(<i>n</i> =15)	Total Mean <i>n</i> ±SD
ePosteriorCranialFossa	Mean±SD	Mean±SD	Mean±SD	Mean±SD	Mean±SD	Mean±SD

Formatted: Font: Tahoma, 8 pt, Bold

Formatted: Right: 0.02", Space Before: 6.8 pt, Line spacing: Multiple 0.93 li

Formatted: Font: Tahoma, 8 pt, Bold

pvalue

<u>Twinningline</u>	<u>Twinningline</u> (mm){TwL}	97.25 \pm 3.18	96.92 \pm 3.11	98.04 \pm 3.57	97.44 \pm 3.45	96.68 \pm 2.72	97.25 \pm 3.210.715 ^a
<u>McRaesline</u>	<u>McRaesline</u> (mm)	32.51 \pm 2.33	32.08 \pm 1.57	32.55 \pm 1.74	32.26 \pm 2	31.98 \pm 1.68	32.26 \pm 1.840.816 ^a
<u>Glivuslength</u>	<u>Glivuslength</u> (mm)	41.54 \pm 2.6	41.31 \pm 1.7	41.88 \pm 1.73	41.74 \pm 2.01	41.65 \pm 2.2	41.59 \pm 1.900.863 ^a
IOP_Oline	<u>OlineOline</u> (mm)	43.37 \pm 2.26	43.68 \pm 2.15	44.21 \pm 1.68	44.39 \pm 2.03	43.89 \pm 1.81	43.9 \pm 2.020.432 ^a
<u>Chamberlainline</u>	<u>Chamberlainline</u> (mm)	75.09 \pm 3.31	76.06 \pm 3.4	75.38 \pm 4	75.13 \pm 4.19	75.62 \pm 3.63	75.51 \pm 3.660.839 ^a
KlausIndex	<u>Klaus'index</u> (mm)	44.74 \pm 2.9	44.32 \pm 1.79	44.49 \pm 1.86	44.5 \pm 2.68	45.13 \pm 2.2	44.57 \pm 2.270.818 ^a
Heightofposteriorfossa	<u>Heightofposteriorfossa</u> (mm)(h)	34.39 \pm 1.6	34.15 \pm 1.47	34.42 \pm 1.55	34.53 \pm 1.47	34.56 \pm 1.19	
		34.37 \pm 1.460.846 ^b					
Heightofsupratentorialregion	<u>Heightofsupratentorialregion</u> (mm)(H)	90.77 \pm 2.05	91.15 \pm 1.81	91.35 \pm 2.08	91.98 \pm 1.96		
		90.67 \pm 1.98	91.24 \pm 1.970.173 ^b				
h/TwL		0.35 \pm 0.02	0.35 \pm 0.01	0.35 \pm 0.02	0.35 \pm 0.02	0.36 \pm 0.01	0.35 \pm 0.020.815 ^a
Posteriorfossavolume	<u>Posteriorfossavolume</u> (cm ³)	164.47 \pm 7.39	161.93 \pm 8.23	163.66 \pm 5.89	162.96 \pm 7.97	158.93 \pm 7.51	
		162.52 \pm 7.640.247 ^b					

IOP-O: Internal Occipital Protuberance; Internal Occipital Protuberance-Opisthion
*ANOVA

Table 4 Comparison of Linear Craniometric Parameters of Posterior Cranial Fossa in between genders

Linear Craniometric Parameters of Posterior Cranial Fossa

^aANOVA

UNDER PEER REVIEW

Table 4 Comparison of Linear Craniometric Parameters of Posterior Cranial Fossa in between genders

<u>Linear Craniometric Parameters of Posterior Cranial Fossa</u>	Female (n=61) Mean \pm SD	Male (n=59) Mean \pm SD	Total Mea n \pm	Total Mean \pm SD
--	--------------------------------	------------------------------	----------------------	------------------------

pvalue	pvalue			
<u>TwinninglineTwinningline</u> (mm){TwL}	95.89 \pm 3.3	98.65 \pm 2.44	97.25 \pm 3.21	$\leq .0001^a$
<u>McRaeslineMcRaesline</u> (mm)	31.57 \pm 1.83	32.97 \pm 1.58	32.26 \pm 1.84	$\leq .0001^a$
<u>ClivuslengthClivuslength</u> (mm)	40.67 \pm 1.49	42.53 \pm 2.02	41.59 \pm 1.99	$\leq .0001^a$
<u>IOP_OlineOline</u> (mm)	43.32 \pm 1.8	44.5 \pm 2.1	43.9 \pm 2.03	0.001^a
<u>ChamberlainlineChamberlainline</u> (mm)	75.42 \pm 3.62	75.61 \pm 3.74	75.51 \pm 3.66	0.785 ^a
<u>KlausIndexKlausIndex</u> (mm)	43.63 \pm 2.05	45.54 \pm 2.08	44.57 \pm 2.27	$\leq .0001^a$
<u>HeightofposteriorfossaHeightofposteriorfossa</u> (mm)(H)	33.57 \pm 1.02	35.21 \pm 1.38	34.37 \pm 1.46	$\leq .0001^a$
<u>HeightofsupratentorialregionHeightofsupratentorialregion</u> (mm)(H)	91.64 \pm 2.03	90.83 \pm 1.84	91.24 \pm 1.97	
0.024^a				
<u>h/TwL</u>	0.35 \pm 0.02	0.36 \pm 0.02	0.35 \pm 0.02	0.028^a
<u>PosteriorfossavolumePosteriorfossavolume</u> (cm ³)	161.53 \pm 6.82	163.54 \pm 8.35	162.52 \pm 7.64	0.151 ^a

A significant p value is denoted in bold

Letters: IOP: Internal Occipital Protuberance-

Opisthion^a:Independent t-test; Letters IOP:-

O: Internal Occipital Protuberance-

Opisthion^a:Independent t-test

Table 5 Analysis of Morphometry of Foramen Magnum

Table 5 Analysis of Morphometry of Foramen Magnum

Shapes of foramen Magnum, Shapes of foramen Magnum Controls(n=120)

Oval	27(22.50%)
Round	24(20%)
Tetragonal	7(5.83%)
Pentagonal	8(6.67%)
Hexagonal	39(32.50%)
Egg	6(5%)
Irregular	9(7.50%)

5,7,7,13–19]. Paraaxial mesodermal insufficiency during embryological development may be responsible for Paraaxial mesodermal insufficiency during

embryological development may be responsible for

development of Chiari malformations [20]. The measure-

development of Chiari malformations [20]. The measure-

ment of TL reflects the anteroposterior distance of PCF, ment of TL

reflects the anteroposterior distance of PCF.

In this study, the mean length of length of TL was 97 was 97.25 \pm 3.21 mm.

In previous literature, the mean length of TL ranges In previous literature, the mean length of TL ranges

from 84.2 to 93.7 mm [from 84.2 to 93.7 mm (7, 21)]. In Chiari malfor-

mations, there is growth in the anteroposterior direction to com-

there is growth in the anteroposterior direction to com-

pensate for the small size of the PCF which results in compensate for the small size of the PCF which results in

higher values of TL [higher values of TL [15, 22]. The length of ML, T

the length of ML, which

Table 6 Analysis of Linear Craniometric Parameters of Foramen Magnum

Linear Craniometric Parameters of Foramen Magnum

Linear Craniometric Parameters of Foramen Magnum

	Controls(n=120)	Range
<u>ForamenMagnumtransversediameter(mm)ForamenMagnumtransversediameter(mm)</u>	27.12 \pm 1.42	23.6–30.1
Foramen	30.99 \pm 2.23	27.6–35.8
<u>MagnumanteroposteriordiameterMagnumanteroposteriordiameter</u> (mm)	691.32 \pm 30.35	632.7–777.7
<u>ForamenMagnumareaForamenMagnumarea</u> (mm ²)		

Formatted: Font: Tahoma, 8 pt, Bold, Character scale: 85%

Table 7 Comparison of Linear Craniometric Parameters of Foramen magnum in different age groups

Linear Craniometric Parameters of Foramen magnum in different age groups of Foramen Magnum

<u>Linear Craniometric Parameters for foramenMagnum</u>	18–30(n=21)	31–40(n=37)	41–50(n=20)	51–60(n=27)	61–70(n=15)	TotalMean \pm SD
Mean \pm SD	Mean \pm SD	Mean \pm SD	Mean \pm SD	Mean \pm SD	Mean \pm SD	n \pm

Formatted: Right: 0.02", Space Before: 6.75 pt, Line spacing: Multiple 0.93 li

Formatted: Font: Tahoma, 8 pt, Bold, Character scale: 85%

Formatted: Font: Tahoma, 8 pt, Bold

<i>p</i> value	<i>p</i> value	<i>p</i> value	<i>p</i> value	<i>p</i> value	<i>p</i> value	<i>p</i> value
Foramen Magnum transverse diameter(mm)	27.03 \pm 1.27	27.08 \pm 1.63	27.24 \pm 1.24	27.59 \pm 1.5	26.36 \pm 0.78	27.12 \pm 1.42 ^a
ForamenMagnumanteroposterior diameter(mm)	31.33 \pm 2.45	30.79 \pm 2.27	30.97 \pm 1.91	31.62 \pm 2.27	29.88 \pm 1.86	30.99 \pm 2.23 ^a
ForamenMagnumanteroposterior diameter(mm)						
Foramen <u>Magnumarea</u> (mm ²)	687.21 \pm 35.4	687.19 \pm 29.02 ^a	698.4 \pm 24.11			
	700.54 \pm 32.81 ^a	681.21 \pm 25.87 ^a	691.32 \pm 30.35 ^a	691.17 ^a	691.32 \pm 30.35 ^a	691.17 ^a

*ANOVA

Table 8 Comparison of linear craniometric parameters of Foramen Magnum in between genders

^aANOVA

UNDER PEER REVIEW

Table 8 Comparison of linear craniometric parameters of Foramen Magnum in between genders

Linear Craniometric Parameters of Foramen Magnum	Male(n=59) Mean \pm SD	Total Mea n \pm SD	Total Mea n \pm SD
Female(n=61) Mean \pm SD			

pvalue	pvalue		
Foramen Magnum transverse diameter	Foramen Magnum transverse diameter (mm)	26.7 \pm 1.27	27.56 \pm 1.44
		27.12 \pm 1.42	0.0008^a
Foramen Magnum anterior-posterior diameter	Foramen Magnum anterior-posterior diameter (mm)	29.94 \pm 1.64	32.07 \pm 2.25
		30.99 \pm 2.23	$\leq .0001^b$
Foramen Magnum area (mm ²)		685.82 \pm 29.59	691.32 \pm 30.35
		697.01 \pm 30.31	0.043^a

^aSignificant pvalue is denoted in bold letters

^bIndependent t-test

Table 9 Analysis of Angular Craniometric Parameters of Posterior Cranial Fossa and Foramen Magnum and Surrounding territory

Significant pvalue is denoted in bold letters

^aIndependent t-test.

Table 9 Analysis of Angular Craniometric Parameters of Posterior Cranial Fossa and Foramen Magnum and Surrounding territory

Angular Craniometric Parameters Controls Angular Craniometric Parameters Controls (n=120) Range Mean \pm SD

ML and CVJ malformations, but usually measurements of ML and CVJ malformations, but usually measurements of ML remains higher in Chiari malformations. The mean length of ML was 32.26 mm in this study. The length of me an length of ML was 32.26 mm in this study. The length of CL is not well documented in the literature. In this study,

Previously well documented in the literature [19, 20, 21, 22, 23, 24]. In this study, the mean length of CL was 75.51 ± 2.66 mm. The mean length of clivus (Cl) and Kline (Kl) (Fig. 4a), which are measures of measures of the size of the basiocciput, vary from 40.4 ± 1.76 mm and 38 ± 4.22 mm, respectively, in the normal population [5, 15, 16, 22, 23–27]. In this study, it was 41 ± 1.99 mm and 49 ± 1.99 mm, respectively.

In this study, the mean length of IOP-

IOP-Oline was 118.3 ± 14.4 mm. The mean length of Oline was 136.89 ± 3.39 mm. The mean length of Clivus (Cl) and Kline (Kl) (Fig. 4a), which are measures of measures of the size of the basiocciput, vary from 40.4 ± 1.76 mm and 38 ± 4.22 mm, respectively, in the normal population [5, 15, 16, 22, 23–27]. In this study, it was 41 ± 1.99 mm and 49 ± 1.99 mm, respectively.

Oli

NBO: Nasion-Basion Opisthion; Nasion-Basion Opisthion

ly. Mean values of Cl and Kl lesser in the patients with Chiari malformations and BII than in the normal population. The IOP-Oline is same measure of supraocciput, and its mean length varies from Kl lesser in the patients with Chiari malformations and BII than in the normal population. The IOP-Oline is same measure of supraocciput, and its mean length varies from 40.9 ± 46.8 mm in the normal population [7, 26]. In this study, the mean length of IOP-Oline was 43.9 ± 2.03 mm.

The height of the posterior fossa is a measure of the shallowness of the posterior fossa, which varies from 30.3 ± 2.03 to 43.9 ± 2.03 mm.

The height of the posterior fossa is a measure of the shallowness of the posterior fossa, which varies from 30.3 ± 2.03 to 43.9 ± 2.03 mm.

agivesmeasureofwidenessoffM, variesfrom32.3to
agivesmeasureofwidenessoffM, variesfrom32.3to
36.21 mm [21, 23]. Although in CVJ malformations,
~~it'ssignificaneit'ssignificance~~ remains inconspicuous, as
previous studies failed to establish the significance between the length of
studies failed to establish the significance between the length of

lowness of the posterior fossa, which varies from 30.3 to 35.2 mm in various studies, probably due to the choice of different landmarks. A decreased height of the posterior fossa denotes a smaller posterior fossa volume (Fig. 4b) which is associated

with Chiari malformations [7, 12, 27]. In this study, it's value was 34.37 \pm 1.46 mm. Twiwise considered compensatory growth of PCF of PCF in the forward

Table 10: Comparison of Angular Craniometric Parameters of Posterior Cranial Fossa, Foramen Magnum and surrounding territory in different age groups

Angular Craniometric Parameters **vs** **Table 10:** Comparison of Angular Craniometric Parameters of Posterior Cranial Fossa, Foramen Magnum and surrounding territory in different age groups

Angular Craniometric Parameters	18–30 (n=21) Mean \pm SD	31–40 (n=37) Mean \pm SD	41–50 (n=20) Mean \pm SD	51–60 (n=27) Mean \pm SD	61–70 (n=15) Mean \pm SD	Total Me \pm Total SD	p value pva ue	
<u>Basal angle</u> <u>Basal angle</u> (°)	125.66 \pm 3.14	125.88 \pm 4.5	125.14 \pm 4.37	127.03 \pm 5.49	125.42 \pm 3.72	125.92 \pm 4.41	0.10	0.633 ^a
<u>Boogard angle</u> <u>Boogard angle</u> (°)	137.4 \pm 4.34	137.54 \pm 3.43	135.12 \pm 2.43	137 \pm 2.84	136.74 \pm 3.44	136.89 \pm 3.39	0.00390	0.118 ^a
<u>NBO angle</u> <u>NBO angle</u> (°)	169.31 \pm 2.38	169.39 \pm 2.09	169.75 \pm 1.24	169.45 \pm 2.08	169.03 \pm 2.1	169.4 \pm 2.01	0.00010	0.884 ^a
<u>Foramen Magnum angle</u> <u>Foramen Magnum angle</u> (°)	12.5 \pm 1.13	12.5 \pm 1.54	13.57 \pm 2.25	13.2 \pm 1.99	12.87 \pm 1.47			
	12.88 \pm 1.74	0.740740	1.148 ^a					
<u>Clivo-edenoid angle</u> <u>Edentoid angle</u> (°)	147.17 \pm 7.72	143.98 \pm 9.23	150.5 \pm 4.97	142.19 \pm 11	146.84 \pm 4.86	145.58 \pm 8.78	0.780	0.012 ^a
<u>Clivopalatal angle</u> <u>Clivopalatal angle</u> (°)	59.83 \pm 5.82	59.48 \pm 5.32	60.76 \pm 5.36	59.82 \pm 6.35	61.59 \pm 6.5	60.1 \pm 5.76	0.760	0.778 ^a
<u>Clivuscanal angle</u> <u>Clivuscanal angle</u> (°)	162.72 \pm 7.85	159.95 \pm 9.74	165.62 \pm 5.11	157.83 \pm 11.39	162.23 \pm 5.65	161.19 \pm 9.02	0.070	0.038 ^a
<u>Clivussupraocciput angle</u> <u>Clivussupraocciput angle</u> (°)	77.82 \pm 5.71	77.31 \pm 3.76	76.86 \pm 4.65	78.66 \pm 4.07	77.09 \pm 5.23			
	77.6 \pm 4.52	0.520520	0.671 ^a					
<u>Tentorial slope</u> <u>Tentorial slope</u> (°)	87.09 \pm 5.94	88.42 \pm 5.44	90.36 \pm 6.07	87.81 \pm 6.5	89.43 \pm 5.26	88.5 \pm 5.87	0.0870	0.416 ^a
<u>Tentorial twinning line angle</u> <u>Tentorial twinning line angle</u> (°)	34.24 \pm 2.25	33.69 \pm 2.47	34.54 \pm 1.66	34.21 \pm 2.07	34.06 \pm 1.68			
	34.09 \pm 2.12	0.120120	0.666 ^a					

^aSignificant values are denoted in bold letters; NBO: Nasion-Basion Opisthoton

^aANOVA

Table 11 Comparison of Angular Craniometric Parameters of Posterior Cranial Fossa, Foramen Magnum and surrounding territory in between genders

Angular Craniometric Parameters As significant

t value is denoted in bold letters NBO Nasion Basion

Opisthion

^aANOVA

UNDER PEER REVIEW

Table 11 Comparison of Angular Craniometric Parameters of Posterior Cranial Fossa, Foramen Magnum and surrounding territory in between genders

<u>Angular Craniometric Parameters</u>	<u>Female(n=6 1) Mean\pmSD</u>	<u>Male(n=59) Mean\pmSD</u>	<u>Total Mea n\pm</u>	<u>Total Mea n\pmSD</u>
--	---	--	--	--

pvalue

	pvalue	pvalue		
<u>Basalangle</u> <u>Basalangle(°)</u>	125.68 \pm 5.24	126.17 \pm 3.37	125.92 \pm 4.41	0.542 ^a
<u>Boogardangle</u> <u>Boogardangle(°)</u>	136.19 \pm 3.02	137.62 \pm 3.63	136.89 \pm 3.39	0.021^a
<u>NBOangle</u> <u>NBOangle(°)</u>	169.07 \pm 1.93	169.75 \pm 2.04	169.4 \pm 2.01	0.061 ^a
<u>ForamenMagnumangle</u> <u>ForamenMagnumangle(°)</u>	12.97 \pm 1.7	12.79 \pm 1.79	12.88 \pm 1.74	0.575 ^a
<u>Clivo-odontoidangle</u> <u>odontoidangle(°)</u>	146.72 \pm 8.63	144.4 \pm 8.84	145.58 \pm 8.78	0.149 ^a
<u>Clivopalatalangle</u> <u>Clivopalatalangle(°)</u>	60.23 \pm 6.23	59.95 \pm 5.27	60.1 \pm 5.76	0.79 ^a
<u>Clivuscanalangle</u> <u>Clivuscanalangle(°)</u>	162.11 \pm 8.82	160.24 \pm 9.29	161.19 \pm 9.07	0.259 ^a
<u>Clivussupraocciputangle</u> <u>Clivussupraocciputangle(°)</u>	77.29 \pm 4.33	77.92 \pm 4.73	77.6 \pm 4.52	0.451 ^a
<u>Tentorialslope</u> <u>Tentorialslope(°)</u>	89.63 \pm 5.82	87.33 \pm 5.73	88.5 \pm 5.87	0.031^a
<u>Tentorialtwinninglineangle</u> <u>Tentorialtwinninglineangle(°)</u>		34.14 \pm 2.09	34.04 \pm 2.17	
	34.09 \pm 2.12	0.794 ^a		

^aSignificant p-value is denoted in bold letters: NBO:Nas

ionBasionOpisthion

*Independent t-test

direction in the case of small

sized PCF [7]

^aSignificant p-value is denoted

in bold letters: NBO:Nas ionBasionOpisthion

*Independent t-test

direction in the case of small sized PCF [7,28], although literature is though literature regarding the significance of this parameter remains scarce. Karagöz F, et al., in their study, showed that the value of h/TwL was reduced (0.26) in patients with Chiari malformations compared to the normal population patients with Chiari malformations compared to the normal population (0.32) [7]. In this study, the mean value of h/TwL ratio was 0.35 \pm 0.02. Various studies have been done to define the values of PFV based on the different auto-mated and manual methods. The range of the values of PFV varies widely, which may be attributed to the differences in the imaging modalities and the possible differences in the segmentation protocols, or the landmarks used in the measurement protocol [1, 2, 5, 7, 12, 29]. In this study, the mean PFV was 162 \pm 7.64 cm³. Chiari mal-formations and BI are most of the times associated with the smaller PCF with the smaller PCF.

Linear craniometric analysis of FM and its clinical implications

Measurements of the FM hold substantial importance in linear craniometric analysis of FM and its clinical implications

Measurements of the FM hold substantial importance in approaching the lesions occupying the PCF and CVJ region. During surgical procedures, information about themorphometry, CVJ region. During surgical procedures, information about themorphometry, morphology, and variations of the FM may affect the surgical outcome and variatio

nsof the FM may affect the surgical outcome.

The Shape of FM has immense clinical significance regarding various surgical approaches. Previous studies have reported differences in the frequency of shapes of FM. It may due to geographical variations, gender and racial differences, etc. The commonest shape of FM described in most of the literatures is oval [30–34]. How-ever, in this study, the most common shape of FM was hexagonal (32.50%), followed by oval (22.50%). Other shapes of FM were round (20.0%), tetragonal (5.83%),

pentagonal(6.67%),irregular(7.50%)and eggshaped and eggshaped(5%).

The anteroposterior and transverse diameters of FM are the valuable parameters used in analysis using variations. FM are the valuable parameters used in analysis of the morphometry of FM. In literature, the anteroposterior and transverse diameters of FM range from 25 to 37 mm and 24 to 35 mm, range from 25 to 37 mm and 24 to 35 mm, respectively [5, 7, 12, 30, 31, 34, 35]. In this study, these measurements were 30.99 ± 2.23 mm and 27.12 ± 1.42 mm, respectively. The measurement of the area of FM is another morphometric tool to analyse FM, whose value of which ranges from 385 to 779 mm², as described in different studies. In this study, it's value was 691 ± 30.35 mm². Usually, there are no differences in the size of FM in different age groups, but males have a larger configuration of FM than females [30–37]. Although patients with Chiari malformations have larger dimensions of FM due to compensatory growth, malformations have larger dimensions of FM due to compensatory growth in the anteroposterior direction, some studies have found no significance in both [37–39]. Muthukumar et al. described importance of anatomical knowledge of FM as necessary for surgical approaches like the transcondylar approach, where drilling of the posterior margin is important to access lesions [31].

Angular craniometric analysis of PCF, FM and surrounding territory and its clinical implications

Evaluation of the craniocervical angles of PCF, FM and CVJ is necessary, as the cranial angles of PCF directly influence the angular geometry of CVJ and consequently the whole vertebral column [6]. BA is routinely used to assess the flattening of skull base, i.e., platybasia. In literature, it's value ranges from 125° to 143° [40]. The mean value in previous studies varies due to the use of the Th

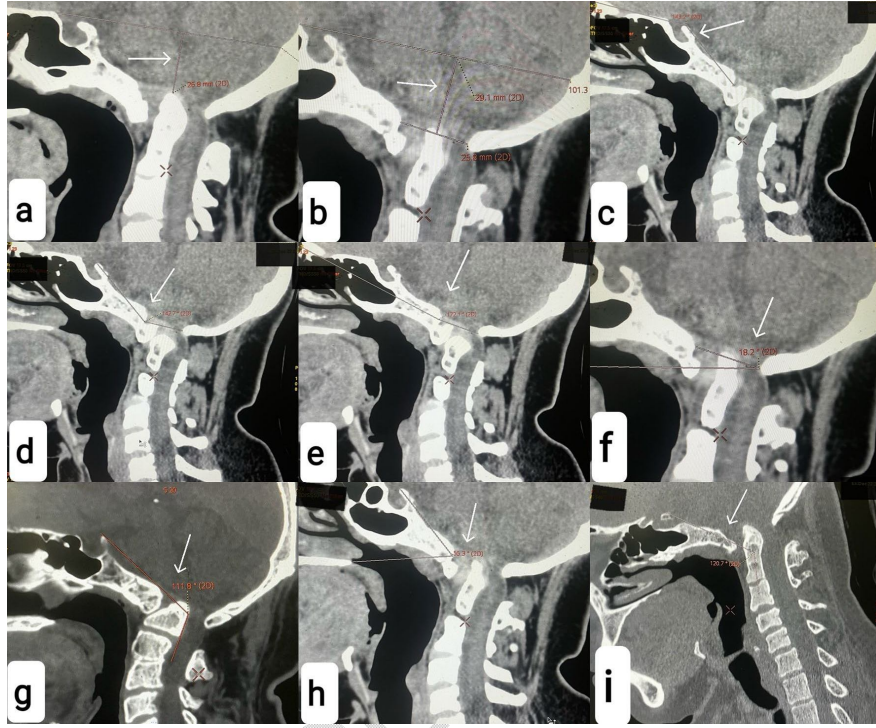


Fig. 4 Midsagittal reconstructed images of computed tomography scan of the posterior fossa and the craniovertebral junction demonstrating the measurements of various craniometric parameters in patients with craniovertebral junction malformations. **a** Klaus index—**4** Midsagittal reconstructed images of computed tomography scan of the posterior fossa and the craniovertebral junction demonstrating the measurements of various craniometric parameters in patients with craniovertebral junction malformations. **a** Klaus index—26.8 mm (decreased), **b** height of posterior fossa—29.1 mm (decreased), **c** Baa angle—Baa angle—143.2° (increased), **d** Bbg angle—Bbg angle—142.7° (increased), **e** Nasion-Basion Opisthion angle—Nasion-Basion Opisthion angle—172.1 (increased), **f** Foramen Magnum Angle—Foramen Magnum Angle—18.2° (increased), **g** Clivus-Canal angle—Clivus-Canal angle—111.8° (increased), **h** Clivopatatal angle—Clivopatatal angle—55.3 (decreased), **i** Clivoodontoid angle—Clivoodontoid angle—120.7° (decreased)

different imaging modalities or ambiguities in the location of landmarks or of landmarks [40, 41]. In this study, the mean value of BA. In this study, the mean value of BA was 125.92° ± 4.41°. Ferreira et al. stated that BA > 129° ± 129° is defined as platybasia with mean value of 116.5° in normal population (Fig. 4c) [41]. BgA and NBO angles are also used for the evaluation of platybasia (Fig. 4d, e). The mean value of BgA ranges from 126°. The mean value of BgA ranges from 126°—137° in the normal population [6, in the normal population [6, 7]. In this study, the mean value of BgA was 136°. In this study, the mean value of BgA was 136°. Botelho et al. found wider BgA in patients with BI (172°) and Chiari malformations (136°) than the control group of the normal population—(126°) and Chiari malformations (136°) than the control group of the normal population—

(126° ± 15.26°) [7]. NBO Angle values vary between 162° and 165°. NBO Angle values vary between 162° and 165° [7, 23, 42]. However, in this study, the mean value of NBO angle was 169.4° ± 2.01°, which was slightly higher than stated in the previous literature. Measurements of BA, BgA and NBO and NBO angles are helpful in diagnosing CVJ malformations like BI and Chiari malformations. All these angles have malformations like BI and Chiari malformations. All these angles have

greater values when measured in the patients with CVJ malformations [6, 7, 23, 41, 42, 44]. A few more angles have been reiterated to complement the diagnosis of BI; FMag is the one of them (Fig. 4f). Its values ranges from 6.21°-11.6° in the normal population, as described in the previous studies. Nascimento et al. Found a much higher value of FMag (25.9° ± 9.3%) in patients with BI than in patients with BI in the normal population [43, 45]. In this study, the mean value of FMag was 12.88 ± 1.74, which was slightly higher than stated in the previous literature. CCA, CPA, COA and CSO are another set of angles that are useful in complementing the diagnosis of CVJ malformations but literature regarding their data and diagnostic value remains scarce. Measurements of these angles are only understood and vary in the previous literatures due to the consideration of the different landmarks or imaging modalities [46-48]. In this study, the mean values of FMag were

CCA, CPA, COA, CSO were 161° CSO were 161°, $19^\circ \pm 9.07^\circ$, 60.1°, 5.76° , 145.58°, 8.78° and 77.6°, $\pm 4.52^\circ$, respectively. Usually, patients with BI, CCA, CPA, COA have lower values than the normal population (Fig. 4 g-i), but the value of CSO of CSO is greater [46–49]. Ma et al. evaluated CPA, COA and CCA and found cut-off values for diagnosing BI, COA and CCA and found cut-off values for diagnosing BI, respectively, at 53.5°, 123.5°, 138.5° [47]. D'AAddario et al. used CSO measurement in the evaluation of fetal posterior fossa and type 2 Chiari malformations, as the values of CSO angle remain constant throughout the posterior fossa and type 2 Chiari malformations, as the value of CSO angle remains constant throughout the gestational age. They found that values of CSO angle decrease in patients with fetal ventriculomegaly related to Chiari malformations [50]. Tentorial slope and TtwA are also measured to assess platybasia [7]. In this study, the mean value of the tentorial slope and TtwA were $88.5^\circ \pm 5.87^\circ$ and $34.09^\circ \pm 2.12^\circ$, respectively. Rehderetal established tentorial slope as an imaging biomarker of the fetal posterior cranial fossa development [51]. Tentorial slope also and TtwA tend to be greater in value in patients with Chiari malformations, but pertaining literature remains controversial with Chiari malformations, but pertaining literature remains controversial [2, 7, 51–53].

To our best knowledge, no previous study has been published in the literature regarding the descriptive analysis. To our best knowledge, no previous study has been published in the literature regarding the descriptive analysis of the morphometry of PCF and FM in the population of the North India. We herein describe different linear and angular craniometric parameters of PCF and FM different linear and angular craniometric parameters of PCF and FM along with their values in this group of the normal population. These values can be taken as reference values while comparing these parameters in patients with CVJ malformations.

Limitations

This study is not without limitations. This study is not without limitations. First, compared with other studies, the sample size is not large enough. Second, we didn't compare the values of different linear and angular craniometric parameters of this part of India with some other territory of India, which could establish the geographical differences between these parameters. Third, we couldn't find the definitive cause of differences in measurements of some parameters. We are looking forward to differences in measurements of some parameters. We are looking forward to performing future studies with

larger samplesize and comparing these findings with those of other geographical regions of India. samplesize and comparing these findings with those of other geographical regions of India.

Conclusions

The fundamental knowledge of the morphology of PCF and PCF and FM is critical in the evaluation of CVJ malformations and surgically approaching these areas. Linear craniometric parameters like ML, CL and Kl are commonly used in the evaluation of BI. Assessment of TL, height of posterior malformations and surgically approaching these areas. Linear craniometric parameters like ML, CL and Kl are commonly used in the evaluation of BI. Assessment of TL, height of posterior cranial fossa, IOP-O length, clival length and PCF volume are important in making the diagnosis of and PCF volume are important in making the diagnosis of

Chiari malformations

Chiari malformations, BA, BgA, NBO are the measures of NB. O are the measures of platybasia and are extensively used in making the diagnosis of BI. FMag, CCA and CPA are relatively newer parameters that are helpful in evaluating BI. This study described almost all the linear and angular craniometric parameters used in the morphometric craniometric parameters used in the morphometric analysis of PCF and PCF and FM. Findings of this study provide the valuable data regarding the linear and angular data regarding the linear and angular craniometric parameters of PCF and FM which could redefine the reference values.

Abbreviations

PCF	Posterior cranial fossa FM
	Foramen magnum fos
saFM	Foramen magnum
CVJ	Craniovertebral junction
L	Twinning line
CVJ	Craniovertebral junction
L	Twinning line
ML	McRae line
CL	Chamberlain line
IOP-O	Internal occipital protuberance opisthion KI
	Klaus' index
IOP-O	Internal occipital protuberance-opisthion KI
	Klaus' index
BA	Basal angle
BgA	Boogard angle
FMag	Foramen magnum angle C
CA	Clivus canal angle
FMag	Foramen magnum angle C
CA	Clivus canal angle
CPA	Clivo palatal angle COA
	Clivodontoid angle
angle COA	Clivodontoid angle
CSO	Clive supraocciput angle
angle TtwA	Tentorial twinning line angle

Availability of CSO

Clivous supraocciput angle
Tentorial twinning line angle

Availability of data and materials

All data that support the findings of this study are available from the neuro-surgery department of Institute of Medical Sciences Banaras Hindu University. Data are however available from the author when requested with permission. All data that support the findings of this study are available from the neuro-surgery department of Institute of Medical Sciences Banaras Hindu University. Data are however available from the author when requested with permission.

Declarations

Ethics approval and consent to participate

Ethics approval and consent to participate

This study was conducted after getting ethical clearance from local institutional ethical committee members. Consent for participation was

obtained from each patient prior to the study obtained from each patient prior to the study.

Consent for publication

Not applicable. We confirm that all data incorporated into this study are anonymized.

Consent for publication

Not applicable. We confirm that all data incorporated into this study are anonymized.

UNDER PEER REVIEW

References

1. Oberman DZ, Baldoncini M, Rabelo NN, Ajler P. Morphometric analysis of posterior cranial fossa and surgical implications. *J Craniovertebr Junction Spine*. 2021;12(2):178-82. https://doi.org/10.4103/jcvjs.jcvjs_205_20.
2. Nishikawa M, Sakamoto H, Hakuba A, Nakanishi N, Inoue Y. Pathogenesis of Chiari malformation: amorphometric study of the posterior cranial fossa. *J Neurosurg*. 1997;86(1):40-7. <https://doi.org/10.3171/jns.1997.86.1.0040>.
3. Wen HT, Rhotor AL Jr, Katsut T, de Oliveira E. Microsurgical anatomy of the transcondylar and heterotranscondylar supracondylar and paracondylar extensions of the far-lateral approach. *Neurosurg and Far-lateral approach*. *J Neurosurg*. 1997;87(4):555-85. <https://doi.org/10.3171/jns.1997.87.4.0555>.
4. Bagley CA, Pindrik JA, Pindrik JA, Bookland MJ, Camara-Quintana JO, Quintana JO, Carson BS. Cervicomedullary decompression for foramen magnum stenosis in achondroplasia. *J Neurosurg: Achondroplasia*. *J Neurosurg*. 2006;104(4 Suppl):166-72. <https://doi.org/10.3171/ped.2006.104.3.166>.
5. Igba S, Robert AP, Mathew D. Computed tomographic study of posterior cranial fossa, foramen magnum, and its surgical implications in Chiari malformations. *Asian J Neurosurg*. 2017;12(3):428-35. <https://doi.org/10.4103/1793-5482.175627>.
6. Potele J, Ferreira FD. Angular craniometry in craniocervical junction. *Bone Jt RVF*. *Ferreira FD. Angular craniometry in craniocervical junction malformation*. *Neurosurg Rev*. 2013;36(4):603-10. <https://doi.org/10.1007/s10143-013-0471-0>.
7. Karagoz F, Igin A, Kapicijoglu SS. Morphometric measurements of the cranium in patients with Chiari type I malformation and comparison with the normal population. *Acta Neurochir (Wien)*. 2002;144(2):165-71. <https://doi.org/10.1007/s007010200020>.
8. Wang S, Zhang DW, Wu K, Fan W, Fan T. Potential association among posterior fossa bone volume and crowdedness (tonsillar hernia, Wang S, Zhang DW, Wu K, Fan T. Potential association among posterior fossa bone volume and crowdedness tonsillar hernia, syringomyelia, and CSF dynamics at the craniocervical junction in Chiari malformation type I and CSF dynamics at the craniocervical junction in Chiari malformation type I. *Front Neurol*. 2023;14:1069861. <https://doi.org/10.3389/fneur.2023.1069861>.
9. Vazquez S, Dominguez JF, Das A, et al. Treatment of Chiari malformations with craniovertebral junction anomalies: where do we stand today? *World Neurosurg X*. 2023;20:100221. <https://doi.org/10.1016/j.wnsx.2023.100221>.
10. Pollock JD, Relleford JH. Population-specific deviations of global human craniovertebral variation from a neutral model. *Am J Phys Anthropol*. *specific deviations of global human craniovertebral variation from a neutral model*. *Am J Phys Anthropol*. 2010;142(1):105-11. <https://doi.org/10.1002/ajpa.21207>.
11. Gova F, Ozma MA, Celik S, Ozma MA, Three-dimensional anatomical landmarks of the foramen magnum for the craniocervical junction. *Craniofac Surg*. 2011;22(3):1073-6. <https://doi.org/10.1097/SCS.0b013e3182107610>.
12. Kanodia C, Parikh VY, Bhatela PR, Sharma DK, Kanodia G, Parikh VY, Sharma DK, Morphometric analysis of posterior fossa and foramen magnum. *J Neurosci Rural Pract*. *analysis of posterior fossa and foramen magnum*. *J Neurosci Rural Pract*. 2012;3(3):261-6. <https://doi.org/10.4103/0976-3147.102602>.
13. Goel A. Basilar invagination, Chiari malformation, Goel A. Basilar invagination, Chiari malformation: a review. *Neuro India*. 2009;57(3):235-46. <https://doi.org/10.4103/0028-3886.53260>.
14. Donnelly IICJ, Munakomi S. *Varacallo M. Basilar Invagination*. [Updated 2023 Feb 12]. Donnelly IICJ, Munakomi S. *Varacallo M. Basilar Invagination*. [Updated 2023 Feb 12]. In: StatPearls [Internet]
15. Schady W, Metcalfe RA, Butler P. The incidence of cranio-cervical bony anomalies in the adult Chiari malformation. *J Neurol Sci*. 1987;82(1-3):193-203. [https://doi.org/10.1016/0022-510X\(87\)90018-9](https://doi.org/10.1016/0022-510X(87)90018-9).
16. Vega A, Quintana F, Berciano J. Basicondrocranial anomalies in adult Chiari malformation: amorphometric study. *J Neurol Sci*. 1990;99(2-3):137-45. [https://doi.org/10.1016/0022-510X\(90\)90150-I](https://doi.org/10.1016/0022-510X(90)90150-I).
17. Yan H, Han X, Jin M, et al. Morphometric features of posterior cranial fossa are different between Chiari malformation with and without syringomyelia. *Eur Spine J*. 2016;25(7):2202-9. <https://doi.org/10.1007/s00586-016-4410-y>.
18. Stovner LJ, Bergan U, Nilsen C, Sjaastad O. Posterior cranial fossa dimensions in the Chiari malformation: relation to pathogenesis and clinical presentation. *Stovner LJ, Bergan U, Nilsen C, Sjaastad O. Posterior cranial fossa dimensions in the Chiari malformation: relation to pathogenesis and clinical presentation*. *Neuroradiology*. 1993;35(2):113-8. <https://doi.org/10.1007/BF00593966>.

19. BotelhoRV,BotelhoPB,HernandezB,SalesMB,RottaJM. Association between brachycephaly, chimaeraformation, and basilarinvagination. *JNeuro SurgACentEurNeurosurg*. 2023;84(4):329-33. <https://doi.org/10.1055/s-0041-1739503>.
20. Marin-PadillaM.Cephalocervicalskeletal-neuraldysraphicdisorders;PadillaM.Cephalocervicalskeletal-neuraldysraphicdisorders;embryology and pathology. *Can J Neurol Sci Neurosci*. 1991;18(2):153-69. <https://doi.org/10.1017/s0317167100031632>.
21. Liu Z, Hao Z, Hu S, Zhao Y, Li M. Predictive value of posterior cranial fossamorphologyinthedecompressionofChiari malformationtypeI;aretro-spectiveobservationalstudy. *fossamorphologyinthedecompressionofChiari malformationtypeI;aretro-spectiveobservationalstudy*. Medicine(Baltimore). 2019;98(19):e15533. <https://doi.org/10.1097/MD.00000000000015533>.
22. Diniz JM, BotelhoRV. Theroleof clivuslengthand cranialbaseflexionangleinbasilarinvaginationandChiari malformationpatho-physiology. *Neurology-NeuroSci*. 2020;41(7):1751-7. <https://doi.org/10.1007/s10072-020-02428-1>.
23. AlkocOA,SongurA,EserOetal.Stereologicalandmorphometric analysisofMRIChiari malformationtype I. *KoreanNeurosurgSoc*. 2015;58(5):454.
24. AlkocOA,SongurA,EserOetal.Stereologicalandmorphometric analysisofMRIChiari malformationtype-I. *KoreanNeurosurgSoc*. 2015;58(5):454-61. <https://doi.org/10.3340/kns.2015.58.5.454>.
25. DoganGM,SigirciA,TetiKB,PasahanR,OncuC,ArslanAK. ComparisonofposteriorcranialfossamorphometricmeasurementsinChiari type I patientswithandwithoutsyringomyelia. *PolRadial*. 2022;87:e694-700. <https://doi.org/10.5114/pjr.2022.123895>.
26. NishikawaM,BolognesiPA,KularWIkunoh,Ohatak Pathogenesisand classificationofChiari malformationtypeIbasedonthemechanismsofptosis;NishikawaM,BolognesiPA,KularWIkunoh,Ohatak Pathogenesisand classificationofChiari malformationtypeIbasedonthemechanismsofptosis;of the brain stem and cerebellum: a morphometric study of the posteriorcranialfossaandcraniovertebralJunction. *JNeuroSurgSkullBase*. 2021;82(3):277-84. <https://doi.org/10.1055/s-0039-1691832>.
27. BogdanovEI,HeissJD,MendelovichEG,MikhaylovIM,HaassA. ClinicalandneuroimagingfeaturesofBogdanovEI,HeissJD,MendelovichEG,MikhaylovIM,HaassA. Clinicalandneuroimagingfeaturesof idiopathic syringomyelia. *Neurology*. 2004;62(5):791-4. <https://doi.org/10.1212/01.wnl.0000113746.47997.ce>.
28. HylandH,KrognessKC.SizeofposteriorfossainChiari typeIinadults. *ActaNeurochirHylandH,KrognessKC.SizeofposteriorfossainChiari typeIinadults*. *ActaNeurochir(Wien)*. 1978;40(3-4):233-42. <https://doi.org/10.1007/BF01774749>.
29. BagciAM,LeeSH,NagornayaN,GreenBA,AlperinN. AutomatedposteriorcranialfossavolumetrybyMRIapplications toChiari malformationtype I. *BagciAM,LeeSH,NagornayaN,GreenBA,AlperinN. AutomatedposteriorcranialfossavolumetrybyMRIapplications toChiari malformationtype I*. *AJR Am J Neuroradiol*. 2013;34(9):1758-63. <https://doi.org/10.3174/ajnr.A3435>.
30. NatsikK,PlagkouM,SkotsimaraC,PlagkosG,SkandalakisP. Amorpho-NatsikK,PlagkouM,SkotsimaraC,PlagkosG,SkandalakisP. Amorpho-metric anatomical and comparative study of the foramen magnumregioninGreekpopulation. *SurgRadiolAnat*. *morpho-metric anatomical and comparative study of the foramen magnumregioninGreekpopulation*. *SurgRadiolAnat*. 2013;35(10):925-34. <https://doi.org/10.1007/s00276-013-1119-z>.
31. MuthukumarN,SwaminathanR,VenkateshG,BhanumathySP. Morphometric analysis of the foramen magnum region as it relates to the transcondylar approach. *MuthukumarN,SwaminathanR,VenkateshG,BhanumathySP*. *to the transcondylar approach*. *ActaNeurochir*. *to the transcondylar approach*. *ActaNeurochir(Wien)*. 2005;147(8):889-95. <https://doi.org/10.1007/s00701-005-0555-x>.
32. AlfaftanM,AlkhaterS,AhaddadF,etal. MorphologicalvariationsandmorphometryAlfaftanM,AlkhaterS,AhaddadF,etal. Morphologicalvariationsandmorphometry

- hometrydetails of the foramen ovale in the Saudi population: a retrospective radiological study. *J Med Life.* 2023;16(3):458-62. <https://doi.org/10.2512/jml-2022-0265>.
33. Prakash KG, Saniya K, Honnegowda TM, Ramkishore HS, Nautiyal A. Morphometric and anatomic variations of foramen ovale in humans skull and its clinical importance. *Asian J Neurosurg.* 2019;14(4):1134-7. https://doi.org/10.4103/ajns.AJNS_243_19
34. Bahçil AdanıSS, OrhanM, et.al. Anatomical evaluation of the foramen magnum conus. *beam computed tomography images and review of literature.* *Cureus.* 2021; 13(11):e19385. Bahçil AdanıSS, OrhanM, et.al. Anatomical evaluation of the foramen magnum conus. *beam computed tomography images and review of literature.* *Cureus.* 2021; 13(11):e19385. <https://doi.org/10.7759/cureus.19385>.
35. Tubbs RS, Crabb PD, Dockery SE, Bartolucci AA, Oakes WJ, Tubbs RS, Eito NS, Grabb P, Dockery SE, Bartolucci AA, Oakes WJ. Analysis of the posterior fossa in children with the Chiari I malformation. *Neurosurgery.* 2001; 48(5):1050-5. <https://doi.org/10.1097/00006123-200105000-00016>.
36. Gardner WJ, Gooldall RJ. The surgical treatment of Arnold-Chiari malformation in adults: an explanation of its mechanism and importance. *encephalography diagnosis. Neurosurgery of encephalography diagnosis.* *J Neurosurg.* 1950;7(3):199-206. <https://doi.org/10.3171/jns.1950.7.3.0199>.

37. Burdan F, Szumilo J, Walocha J, et al. Morphology of the foramen magnum in young eastern European adults. *Folia Morphol (Warsz)*. 2012;71(4):205-16.
38. Bogdanović Fažudinova AT, Heiss JD. The small posterior cranial fossa syndrome and chiari malformation type 0. *J Clin Med Bogdanović Fažudinova AT, Heiss JD*. The small posterior cranial fossa syndrome and chiari malformation type 0. *J Clin Med*. 2022;11(18):5472. <https://doi.org/10.3390/jcm11185472>.
39. Furtado SV, Thakre DJ, Venkatesh PK, Reddy K, Hegde AS. Morphometric analysis of foramen magnum dimensions and intracranial volume in pediatric Chiari I malformation. *Acta Neurochir (Wien)*. 2010;152(2):221-7. <https://doi.org/10.1007/s00701-009-0480-5>.
40. Koenigsberg RA, Vaki N, Hong TA, et al. Evaluation of platybasia with MR imaging. *AJR Am J Neuroradiol*. Koenigsberg RA, Vaki N, Hong TA, et al. Evaluation of platybasia with MR imaging. *AJR Am J Neuroradiol*. 2005;26(1):89-92.
41. Ferreira JA, Botelho RV. Determination of normal values of the basilar angle in the era of magnetic resonance imaging [published correction appears in *World Neurosurg* 2020 Apr; 136:480]. *World Neurosurg*. World Neurosurg. 2019;132:363-7. <https://doi.org/10.1016/j.wneu.2019.09.056>.
42. Adam AM. Skull radiograph measurements of normals and patients with basilar impression: use of Landzert's angle. *Surg Radiol Anat*. 1987;9(3):225-9. Adam AM. Skull radiograph measurements of normals and patients with basilar impression: use of Landzert's angle. *Surg Radiol Anat*. 1987;9(3):225-9. <https://doi.org/10.1007/BF02109633>.
43. Nascimento JJC, Silveira M, Ribeiro ECO, Neto EJS, Nascimento JJC, Silveira M, Ribeiro ECO, Neto EJS, Araújo A, Neto SA, Diniz PRB. Foramen magnum angle: a new parameter for basilar invagination of type B. *World Neurosurg*. Foramen magnum angle: a new parameter for basilar invagination of type B. *World Neurosurg*. 2021;152:121-3. <https://doi.org/10.1016/j.wneu.2021.06.028>.
44. Silva ATPB, Silva LTPB, Vieira AENP, et al. Craniometric parameters for the evaluation of platybasia and basilar invagination on magnetic resonance imaging. *Silva ATPB, Silva LTPB, Vieira AENP, et al. Craniometric parameters for the evaluation of platybasia and basilar invagination on magnetic resonance imaging: a reproducibility study*. *Radiol Bras*. 2020;53(5):314-9. <https://doi.org/10.1590/0100-3984.2019.0068>.
45. Jian Q, Zhang B, Jian Bo X, Chen Z. Basilar invagination: at it of the foramen magnum [published correction appears in *World Neurosurg* Jian Q, Zhan gB, Jian Bo X, Chen Z. Basilar invagination: at it of the foramen magnum [published correction appears in *World Neurosurg* 2022 Nov;167:255]. *World Neurosurg*. World Neurosurg. 2022;164:e629-35. <https://doi.org/10.1016/j.wneu.2022.05.027>.
46. Nagashima C, Kubota S. Craniovertebral abnormalities: Modern diagnosis and a comprehensive surgical approach. *Neurosur Rev*. 1983;6(4):187-97. Nagashima C, Kubota S. Craniovertebral abnormalities: Modern diagnosis and a comprehensive surgical approach. *Neurosur Rev*. 1983;6(4):187-97. <https://doi.org/10.1007/BF01743100>.
47. Ma L, Guo L, Li X, et al. Clivopatula angle: a new diagnostic method for basilar invagination on magnetic resonance imaging. *Eur Radiol*. method for basilar invagination on magnetic resonance imaging Eur Radiol. 2019;29(7):3450-7. <https://doi.org/10.1007/s00330-018-5972-3>.
48. Xu S, Gong R. Clivodens Angle: A New Diagnostic Method for Basilar Invagination on Computed Tomography Spine (PhD Pa1976).
49. Xu S, Gong R. Clivodens Angle: A New Diagnostic Method for Basilar Invagination on Computed Tomography Spine (PhD Pa1976). 2016;41(17):1365-71. <https://doi.org/10.1097/BR.0000000000001509>.
50. Basaran R, Efendioglu M, Senol M, Ozdogan S, Isik N. Morphometric analysis of posterior fossa and craniovertebral junction in subtypes of Chiari I malformation. *Clin Neurosurg*. 2018;169:1-11. <https://doi.org/10.1016/j.clineuro.2018.03.017>.
51. D'Addario V, Pinto V, Del Bianco A, et al. The clivus-supraocciput angle: a useful measurement to evaluate the shape and size of the fetal posterior fossa and to diagnose Chiari I malformation. *Ultrasound Obstet Gynecol*. 2001;18(2):146-9. D'Addario V, Pinto V, Del Bianco A, et al. The clivus-supraocciput angle: a useful measurement to evaluate the shape and size of the fetal posterior fossa and to diagnose Chiari I malformation. *Ultrasound Obstet Gynecol*. 2001;18(2):146-9.

- 6-9. <https://doi.org/10.1046/j.1469-0705.2001.00409.x>.
51. RehderR,YangF,CohenAR.Variationsoftheslopeofthetentoriumdur-ingchildhood.*ChildsNervSyst.*2016;32(3):441-50.<https://doi.org/10.1007/s00381-015-2899-8>.
52. KaoSC,WaziriMH,SmithWL,SatoYYuhWT,FrankenEA.MRIimaging.KaoSC,WaziriMH,SmithWL,SatoYYuhWT,FrankenEA.MRIimagingofthe cranivertebral junction, cranium, and brain in children with chondroplasia. *AJRAmRoentgenolwithachondroplasia.AJRAmRoentgenol*1989;153(3):565-9. <https://doi.org/10.2214/ajr.153.3.565>.
53. MilhoratTH,ChouMW,TrinidadEM,etal.Chiarimalformationredefined.MilhoratTH,ChouMW,TrinidadEM,etal.Chiarimalformationredefined: clinical and radiographic findings for 364 symptomatic patients. *Neurosurgery*.1999;44(5):1005-17. <https://doi.org/10.1097/00006123-199905000-00042>.